POLITECNICO DI TORINO
Repository ISTITUZIONALE

Impact of Wind-Wave Misalignment and Wave Directionality on Fatigue Damage of Floating Wind Turbines

Original
Impact of Wind-Wave Misalignment and Wave Directionality on Fatigue Damage of Floating Wind Turbines / Mangia, G., Giorgi, G., Bracco, G.. - 7A: Ocean Renewable Energy:(2026). (OMAE 2026: ASME 2026 45th International Conference on Ocean, Offshore and Arctic Engineering Tokyo (JPN) June 7–12, 2026) [10.1115/omae2026-177061].

Availability:
This version is available at: 11583/3016144 since: 2026-09-30T09:43:10Z

Publisher:
ASME

Published
DOI:10.1115/omae2026-177061

Terms of use:

This article is made available under terms and conditions as specified in the corresponding bibliographic description in the repository

Publisher copyright

(Article begins on next page)

09 November 2026

Proceedings of the ASME 2026 45th International Conference on Ocean, Offshore, and Arctic Engineering
OMAE2026
June 7-12, 2026, Tokyo, Japan

OMAE2026-177061

IMPACT OF WIND-WAVE MISALIGNMENT AND WAVE DIRECTIONALITY ON FATIGUE DAMAGE OF FLOATING WIND TURBINES

Gabriele Mangia[1,*], Giuseppe Giorgi[1], Giovanni Bracco[1],

[1]Marine Offshore Renewable Energy Lab, Politecnico di Torino, Turin, Italy

ABSTRACT

Ongoing climate change and worldwide policies are driving a shift towards low-carbon electricity generation. Within this context, offshore wind energy plays a pivotal role. To extend the use of wind turbines in deep waters, floating systems have recently been proposed and tested in pre-commercial installations. However, the harsh marine environment poses significant structural challenges, especially for long-term reliability. Appropriate fatigue design is therefore crucial to ensure safety and to avoid costly emergency maintenance operations. Significant uncertainty remains in modeling the wind and wave climate and their impact on the fatigue life of floating wind turbines, particularly regarding wave directional spreading and wind–wave misalignment. Hence, the focus of this work is to evaluate their influence on the fatigue damage at the interface between tower and transition piece for the IEA 15 MW reference turbine coupled with the VolturnUS semisubmersible platform. Results show that the wind-wave misalignment has a significant impact on fatigue damage, because of the different behavior of the platform for several wave directions and its interaction with the wind field. Moreover, when considering wave directional spreading, preliminary results indicate that the fatigue damage associated to the mean wave direction decreases, while increasing across the full range of investigated directions.

Keywords: Fatigue, Wave Multidirectionality, Misalignment, Floating wind

NOMENCLATURE

Roman letters

A	Tower base area
BEM	Boundary Element Method
DEL	Damage Equivalent Load
DLC	Design Load Case
H_s	Significant wave height
I_x, I_y	Tower base moments of inertia
k	Thickness exponent
$\log \bar{a}$	Intercept of $\log N$ axis
N	Maximum Number of cycles before failure
N_{rf}	Total number of σ cycles detected by RA
NSS	Normal Sea State
NTM	Normal Turbulence Model
RA	Rainflow Algorithm
RAO	Response Amplitude Operator
t	Thickness
T_p	Peak period
t_{ref}	Reference thickness
$TwrBsMxt$	Tower base Moment on the x-axis
$TwrBsMyt$	Tower base Moment on the y-axis
$TwrBsFzt$	Tower base force on the z-axis
V	Mean wind speed

Greek letters

β	Tower Base angle
ϑ	Wave direction angle
σ	Stress
ω	Frequency

Superscripts and subscripts

a	Amplitude
i	i_{th}
m	Mean

1. INTRODUCTION

The interest in offshore wind energy is continually increasing, propelled by investments focused at reducing the carbon intensity of electricity generation. Bottom-fixed farms have seen a boost in successful installations, particularly in the North Sea, where shallow seabeds are favorable to this technology. However, the need to access valuable resource sites characterized by deeper bathymetries has led to the development of floating technologies. Ensuring the reliability and safety of floating wind turbines requires rigorous design. These tests also encompass fatigue life checks to guarantee the product's durability and performance under cyclic loading. Most of the literature work concerning fatigue

*Corresponding author: gabriele.mangia@polito.it
Documentation for `asmeconf.cls`: Version 1.43, March 11, 2026.

Copyright ©2026 by ASME

is based on DNV-ST-0437 [1], a DNV standard where several Design Load Cases (DLCs) are reported, each of them focusing on extreme loads, fatigue loads or both. In particular, when it comes to fatigue evaluation in normal operating conditions the DLC 1.2 is applied. This load case requires wind Normal Turbulence Model (NTM) and Normal Sea State (NSS) for waves. Wind-wave misalignment and wave multidirectionality should be taken into account in the evaluation. Previous studies in the offshore wind sector regarding these two conditions have investigated their effect on loads and fatigue damage.

For the misalignment between wind and wave in [2] is reported that considering only the unidirectional wind-wave case for floating structures leads to an underestimation of tower base side-to-side bending moment up to 50% while a slight overestimation (5%) of the fore-aft bending moment is predicted. For these reasons, the authors recommend the integration of the analysis for 90° wind-wave misalignment to capture fatigue characteristics. In [3], the maximum fatigue damage at the tower base in misalignment conditions is found to be lower than the aligned case for several floating platforms. In [4] the misalignment contributes to an increase of the standard deviation of the roll bending moment, while no significant trend is present in the pitch bending moment. Concerning the wave multidirectionality, in [5] a reduction up to 60 % in fatigue damage is forecast when wave multidirectionality is introduced. On the other hand, in [6], sway and roll motions are introduced with multidirectional sea-states, roughly equal to 20% of pitch and surge motions. Additional analyses on fatigue and extreme loads are therefore recommended.

FIGURE 1: UMaine VolturnUS-S platform designed for the IEA-15-240 RWT system [7].

2. METHODOLOGY

The turbine used in this work is the IEA 15 MW coupled with the open source semisubmersible platform UMaine VolturnUS-S [7]. This configuration (figure 1) is among the most studied in literature.

To evaluate the effect of wind-wave misalignment and the multidirectionality of waves, aero-servo-elastic simulations were performed using the software OpenFAST [8], a tool developed by NREL and representing the state of the art of aero-servo-elastic simulations of offshore wind turbines. In particular, three types of simulations were conducted for each triplet of environmental conditions, namely mean wind speed (V), significant wave height (Hs) and wave peak period (Tp):

- Aligned wave and wind directions, representing collinear sea states;
- Misaligned wave and wind directions, with relative offsets of 30°, 60°, and 90°;
- Aligned wave and wind directions, but with the wave field characterized by directional spreading about the mean direction of ±90°, and spreading coefficients equal to 1, 5 and 10.

2.1. Simulations setup

In order to run the simulations, OpenFAST requires as input the hydrodynamic coefficients of the system and the excitation forces for several frequencies and directions, as well as a three-dimensional turbulent wind field. Concerning hydrodynamics, the calculations were performed using Nemoh [9], a BEM solver that evaluates the hydrodynamic coefficients and excitation forces. Within the framework of linear potential flow theory, these hydrodynamic quantities are independent of the specific sea state and depend only on the body geometry, water depth, wave frequency, and wave direction. In figure 2, the orientation of the platform is represented.

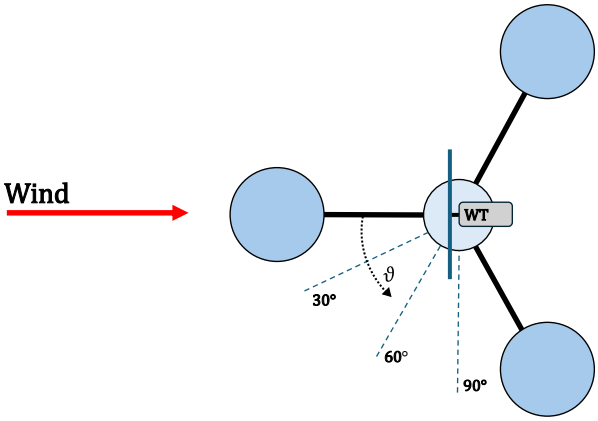

FIGURE 2: Orientation of the platform and mean wind direction.

Copyright ©2026 by ASME

TABLE 1: Triplets selected for the simulations.

Mean Wind Speed 'V'	Wave Significant Height 'H_s'	Wave Peak Period 'T_p'
7 m/s	1.5 m	7 s
7 m/s	1.5 m	11 s
11 m/s	1.5 m	7 s
11 m/s	2.5 m	11 s
15 m/s	2.5 m	7 s
15 m/s	2.5 m	11 s
19 m/s	2.5 m	7 s
19 m/s	4.5 m	11 s

The wind field is provided through Turbsim [10], a stochastic full-field wind simulator able to generate turbulent wind velocity fields to be used in aeroelastic simulations. It employs turbulence models and spatial coherence functions. A turbsim file was created for each mean wind speed associated to the chosen triplets. In Table 1 the triplets used in the simulations are reported. They are chosen among the possible combination of mean wind speed V, significant height H_s and peak period T_p characterizing a random point in the Atlantic Ocean. In particular, the four mean wind speeds are selected to be lower, around and higher than the rated speed of the turbine, to be as much representative as possible of all the control phases of the turbine and consequently of the aerodynamic forces acting on the structure.

The initial portion of OpenFAST simulations is discarded to remove transient effects. The remaining response corresponds to a minimum duration of 10 minutes, in accordance with IEC 61400-1 recommendations [11]. For design purposes, the standard also recommends six realizations associated to this length, thus reaching one hour simulations. However, as shown in [12], the total simulation length has a negligible influence on the Damage Equivalent Loads (DELs) of tower base bending moments. Therefore, the adopted duration is considered sufficient for the purposes of the present comparative study and allows for lower computational costs. For the simulations including the directional spreading, wave loading is modeled using the directional wave formulation implemented in OpenFAST. The wave field is described by a frequency–direction spectrum $S(\omega, \vartheta)$, expressed as the product of a one-dimensional wave spectrum $S(\omega)$ and a directional spreading function $D(\vartheta)$:

$$S(\omega, \vartheta) = S(\omega)\, D(\vartheta). \tag{1}$$

The directional spreading function distributes the wave energy around the mean propagation direction and is defined in OpenFAST through a cosine-power spreading model. Its shape is controlled by a spreading coefficient: higher values represent more directionally concentrated wave fields, while lower values stand for broader directional distributions.

The continuous directional spectrum is discretized into a finite number of wave directions (in these simulations 13 directions are chosen) selected to ensure an adequate angular resolution while maintaining computational efficiency. Each directional component is assigned a fraction of the total spectral energy according to the prescribed spreading function, such that the target wave spectrum is preserved. The directional spreading is defined over the angular range ±90° centered on the mean wave direction.

2.2. Simulations post-processing

A matlab code is used in order to postprocess the outputs of openFAST and obtain the fatigue damage at the tower base. From ElastoDyn module the x, y and z components of both the moment and the force at the tower base can be retrieved. In particular, TwrBsMxt, TwrBsMyt and TwrBsFzt are required to calculate the axial stress acting at the tower base using equation 2,

$$\sigma_z = \frac{F_z}{A} + \frac{M_x R \sin\beta}{I_x} - \frac{M_y R \cos\beta}{I_y} \tag{2}$$

where F_z, M_x, M_y are the axial force and X-axis and Y-axis moments at the base of the tower, β and R are the angle and the external radius of the section at which the stress is calculated, I_x and I_y are the inertia moments of the section. In figure 3 the coordinates at the tower base are shown.

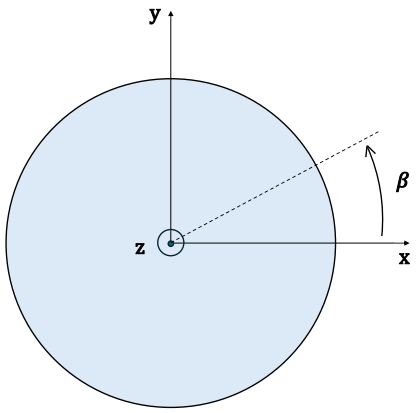

FIGURE 3: Tower base coordinates.

For each timestep of the simulation the axial stress is calculated at several angles β of the tower. The hourly stress timeseries is then analyzed through the Rainflow algorithm: this procedure is necessary to convert the stress time series into stress cycles that can be used to evaluate the fatigue damage. This algorithm generates as output the mean stress σ_m, the stress amplitude σ_a and the associated number of cycles n_{σ_a,σ_m}. These values can

Copyright ©2026 by ASME

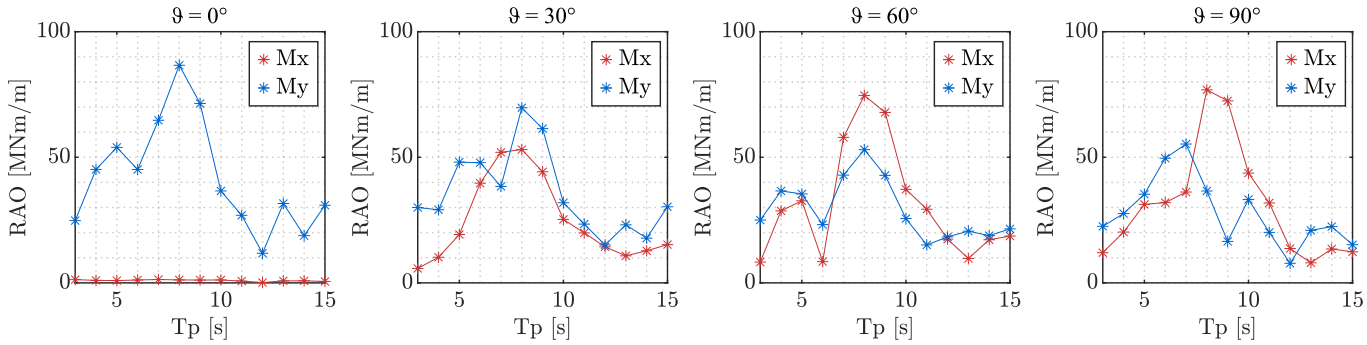

(a) Tower base moments.

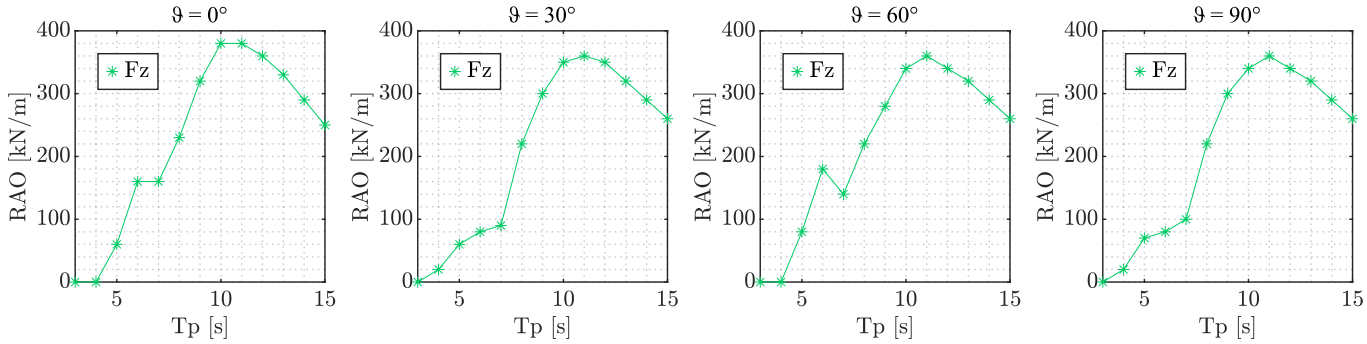

(b) Tower base axial force.

FIGURE 4: RAO of tower base moments and axial force for each misalignment angle.

be used to enter the S-N curves and to evaluate the damage associated to each cycle. For this work, the S-N curves adopted in the standard DNV-RP-C203 [11] are used, in particular the 'D' curve related to transverse butt welds, welded from both side. Equation 3 shows the final formula,

$$\log N = \log \bar{a} \; - m \log \left(\sigma_a \left(\frac{t}{t_{ref}} \right)^k \right) \tag{3}$$

where N is the maximum number of cycles before failure associated to σ_a, $\log \bar{a}$ is the intercept of $\log N$ axis, $t_{ref} = 25$ mm is the reference thickness, t is the thickness at which the crack grows (here the outer surface is assumed) and $k = 20$ mm is the thickness exponent for the selected typology of welding.

The reduction effect generated by the mean stress is not accounted to be conservative, as also recommended by the standard in case of residual stresses due to weldings; hence, only σ_i will be used from this point on in the nomenclature. Using equation 3, the maximum number of cycles for all the σ_a detected by the Rainflow algorithm is found, and then used to obtain the total damage induced during the simulation through Miner's rule [12, 13] reported in equation 4,

$$D = \sum_{i=1}^{N_{rf}} \frac{n_{\sigma_i}}{N_{\sigma_i}} \tag{4}$$

where n_i are the number of cycle performed for a stress σ_i, N_i is the maximum number of cycles for the same stress σ_i and N_{rf} is the total number of σ detected by the Rainflow algorithm.

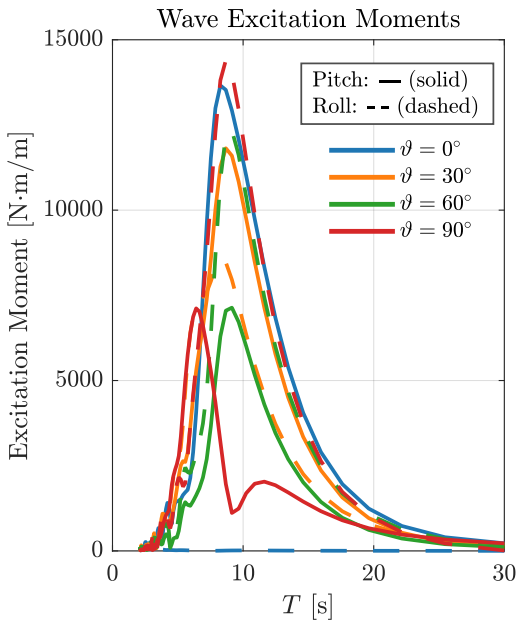

FIGURE 5: Excitation moments from Nemoh: Pitch and Roll.

Copyright ©2026 by ASME

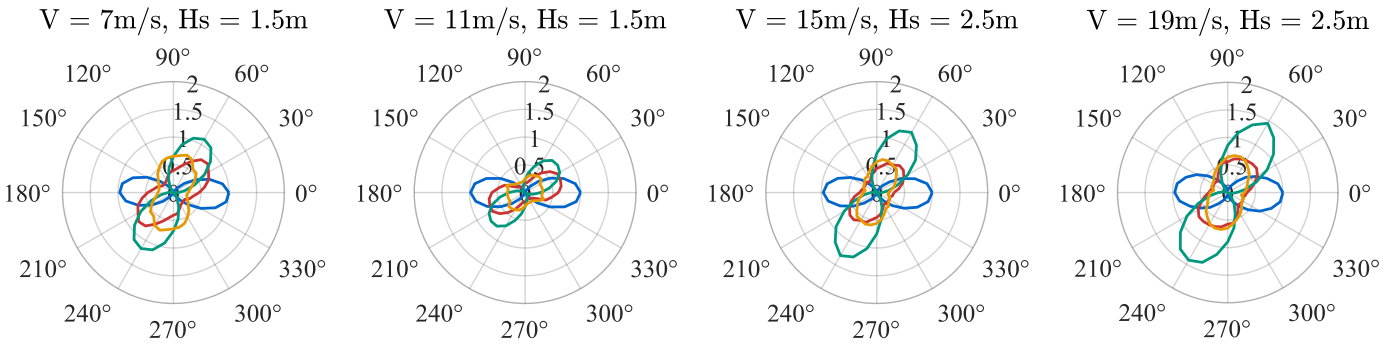

(a) T_p = 7 s.

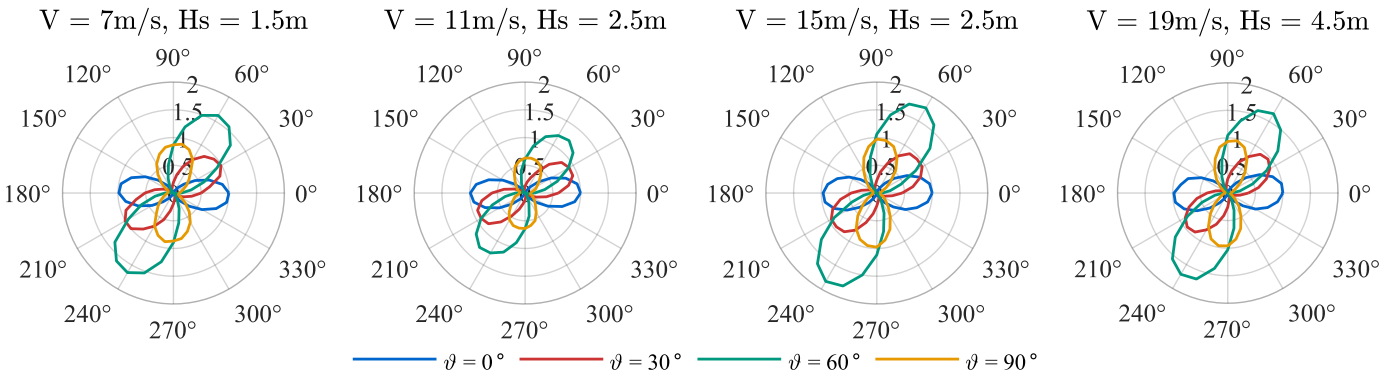

(b) T_p = 11 s.

FIGURE 6: Tower base normalized hourly damage: wind-wave misalignment effects.

3. RESULTS

3.1. M_x, M_y and F_z RAO analysis

Before starting the analysis of the several configurations, the Response Aplitude Operators (RAOs) of the x-axis and y-axis moments, as well as the force acting on the z-axis are analyzed, in order to understand if there are directions or periods for which the system shows higher response without accounting for the wind effect (figure 4). They are obtained from time-domain simulations under regular wave excitation only, with no wind and with the rotor not operating. The structural model includes the tower flexibility, and therefore the computed RAOs account for the elastic response of the tower. It is possible to notice that for all misalignment angle, the M_y RAO exhibits a peak between 7 – 8 s, while M_x is negligible for $\vartheta = 0°$ and shows a peak at 8 s in the remaining cases. These trends, and in particular the peaks, are in accordance with the Nacelle Fore-aft and Pitch RAO in NREL report [7]. The increase in the bending moments is therefore associated with the amplified platform oscillations occurring in the 7 – 8 s range, which could lead to a higher component of gravitational loads. For the sake of completeness, the wave excitation moments acting on the pitch and roll degrees of freedom have also been analyzed and are reported in figure 5. The results show that the pitch degree of freedom is consistently excited by wave loading, even when waves propagate along the y-axis. In contrast, waves propagating along the x-axis do not induce significant excitation moments in roll. This behavior is consistent with the trends observed in the tower base bending moment RAOs and further increase the confidence in the coupling between platform rotational motions and tower base fatigue response. Concerning the axial force F_z, the peak at around 11 s is in accordance with the local peak in the heave RAO of [7]. This appears to be reasonable, as in absence of wind the trend should be mostly dependent on the hydrodynamic characteristics of the system and it is also confirmed by the similarity of the system behavior for each misalignment angle ϑ. It is also possible to notice that no excitation of the first bending moment of the tower is shown both in M_x and M_y RAOs. The wave periods considered for their computation were selected to cover the relevant armonics of the JONSWAP spectrum, associated with the two analyzed peak periods (7 and 11 seconds). The first bending modes of the tower are characterized by higher natural frequencies, which correspond to periods of approximately 2 seconds [7]. As a consequence, no significant modal excitation of the first tower bending modes is observed in the reported RAOs.

3.2. Wind-Wave misalignment effects

In figure 6 it is possible to see the effect of the combined action of wind and wave on the structure related to the aforemen-

Copyright ©2026 by ASME

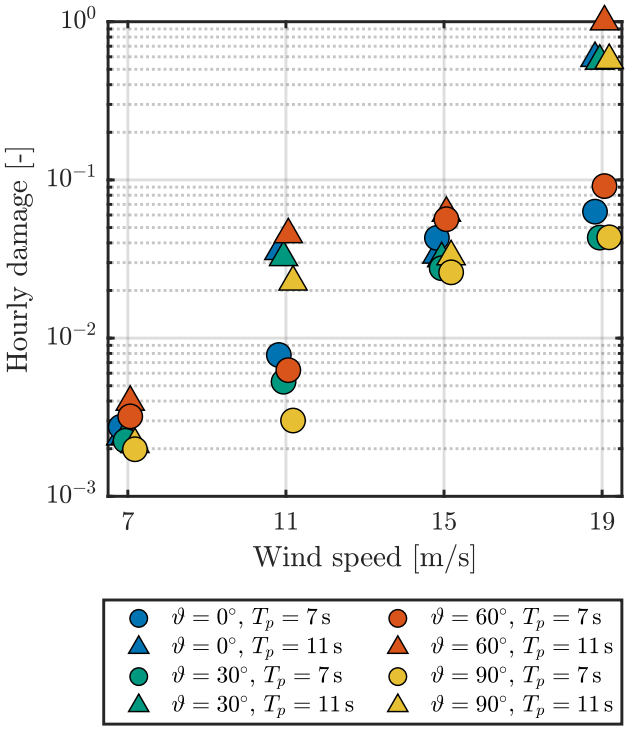

FIGURE 7: Comparison of normalized hourly maximum damage for all the triplets.

tioned triplets. The polar plots illustrate the tower base section at several β angles, for which the hourly damage is computed and subsequently normalized with respect to the maximum damage corresponding to the aligned wind–wave case ($\vartheta = 0°$). For almost the totality of the simulations, the highest damage is associated to a misalignment angle β of 60°. This appears to be related to the geometrical characteristics of the structure that reports two external columns aligned perpendicularly to wave direction. The only case in which there is a prevalence in another direction is the triplet '$V = 11$ m/s, $H_s = 1.5$ m, $T_p = 7$ s', where the highest damage is associated to the aligned case. The anomaly of this behavior may be explained by both the higher hydrodynamic excitation already discussed for figure 4 and by the proximity to the rated speed and the change in the aerodynamic response of the turbine. Nevertheless, more investigation is required to deeply understand the exact reason of this behavior. Moreover, it is possible to notice that for $T_p = 7$ s the damage for $\beta = 30°, 60°$ is spread more uniformly across the section with respect to the remaining cases. This may be due to a more similar contribution of the two tower base moments and the axial force to the damage of the structure.

Figure 7 presents the maximum fatigue damage resulting from each combination of environmental triplet and wind–wave misalignment. The damage values are normalized with respect to the maximum damage observed across all simulations, which corresponds to $V = 19$ m/s, $H_s = 4.5$ m, $T_p = 11$ s, and $\vartheta = 60°$. For clarity, only wind speed V and peak period T_p are explicitly indicated, while the corresponding significant wave height H_s for each triplet is reported in table 1. It can be observed that, for $V = 11$ m/s and $V = 19$ m/s, the fatigue damages associated with the two considered peak periods exhibits a clear separation, driven by the different values of H_s. Higher H_s values correspond to increased wave energy content and, consequently, to higher fatigue loading. For $V = 7$ m/s and $V = 15$ m/s, higher T_p is generally associated with increased damage; however, the difference between the two peak periods associate damages is trivial. In order to better isolate the relative contribution of wave- and wind-induced loads, additional simulations have been carried out. Since no significant variation in fatigue damage is observed among environmental triplets that differ only for T_p (as shown in figure 7), this additional analysis is restricted to triplets having $T_p = 11$ s. For all the wind speed already analyzed, simulations having $H_s = 1.5/2.5/4.5$ m have been carried out.

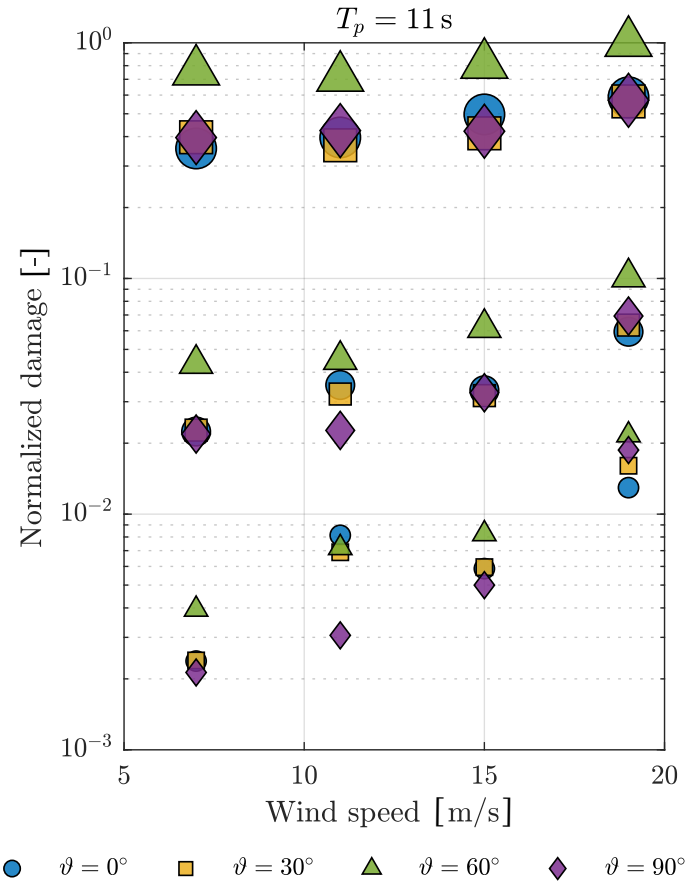

FIGURE 8: Additional analysis on wave and wind influence on fatigue damage. Marker size is proportional to $H_s = 1.5/2.5/4.5$ m

.

As illustrated in figure 8, increasing values of H_s lead to a reduced relative influence of wind, as the fatigue response is increasingly dominated by wave loading. Conversely, for low H_s (e.g., $H_s = 1.5$ m), the effect of the control system and of wind turbulence become evident, producing a peak of damage at the rated speed and then an ever increasing trend towards the highest

Copyright ©2026 by ASME

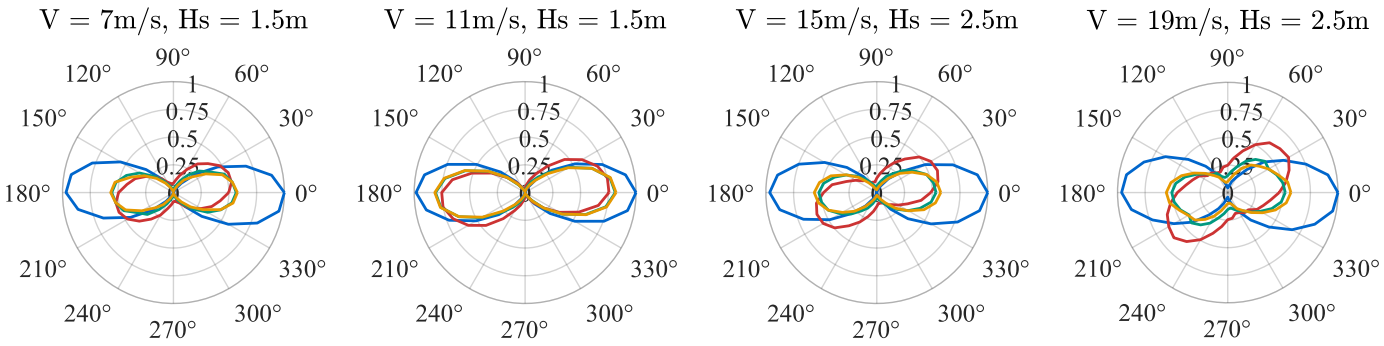

(a) T_p = 7 s.

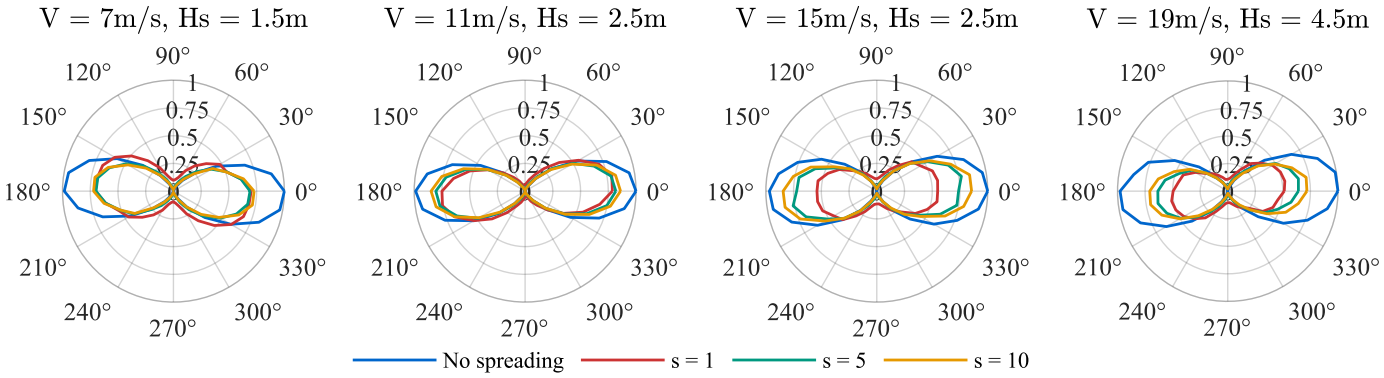

(b) T_p = 11 s.

FIGURE 9: Tower base normalized hourly damage: directional spreading effects.

wind speeds.

3.3. Wave directional spectrum effects

In figure 9 the hourly damages associated to several spreading coefficients are plotted. Similarly to the misalignment cases, some differences exist between the triplets having T_p = 7 s and those having T_p = 11 s. As expected, the higher damage is registered for directional sea states, where no spreading function is used. However, despite a wind-mean wave direction alignment, for T_p = 7 s and less directional sea states (s = 1) the most damaging direction goes towards β = 210°. This can be explained considering figure 4 a: for ϑ = 30° (considering tower coordinates, β = 210°) higher average values of the RAOs associated with the bending moments M_x and M_y are observed in the vicinity of T_p = 7 s, where the wave spectrum is concentrated. In addition to this, the directional spectrum shows higher energy content for directions closer to the mean one, hence the peak damage is shifted from ϑ = 60° to lower values. Viceversa, for sea states having T_p = 11 s (figure 4 b), lower values of the RAOs are associated in the vicinity of the peak period of the wave spectrum, hence the fatigue is driven strongly by the mean wave direction and by wind turbulence.

4. CONCLUSIONS

In this work, the influence of wind - wave misalignment and wave spreading on the fatigue behavior of a floating offshore wind turbine tower base has been analyzed. The RAOs of the moments have shown an higher level of excitation for T_p = 7 s which resulted in a more difficult interpretation of the results concerning triplets having the same peak period. It is noteworthy that the higher damage is registered along the tower base angle coincident to the wave direction and that in almost all the cases, a misalignment β = 60° seems to be the most detrimental for the analyzed section. This result is probably driven by the orientation of the platform, showing higher damage when two external columns are aligned and perpendicular to the incident wave direction.

The maximum damage is registered for V = 19 m/s, H_s = 4.5 m, T_p = 11 s, ϑ = 60°, and simulations have shown that the maximum damage of the tower base section is strongly affected by the sea-state and increases for increasing H_s. The same trend is shown for increasing V and T_p even though with lesser impact.

Concerning the introduction of wave directional spreading in the simulations, a reduction of the maximum hourly damage for the tower base section is found for all the analyzed triplets. To conclude, this work shows that without considering wave direc-

Copyright ©2026 by ASME

tional spreading, some variations may occur in the most damaged angle of the tower section; however considering unidirectional waves leads to conservative fatigue estimations. On the other hand, not considering wind-wave misalignment may lead to a not conservative fatigue calculation and the orientation of the platform appears to be significantly meaningful for the simulation results.

ACKNOWLEDGMENTS

This publication is part of the project PNRR-NGEU which has received funding from the MUR – DM 117/2023.

REFERENCES

[1] GL, DNV. "STANDARD DNV GL ST 0437: Loads and Site Conditions for Wind Turbines." *DNV GL: Oslo, Norway* (2016).

[2] Barj, Lucie, Jonkman, Jason M, Robertson, Amy, Stewart, Gordon M, Lackner, Matthew A, Haid, Lorenz, Matha, Denis and Stewart, Susan W. "Wind/wave misalignment in the loads analysis of a floating offshore wind turbine." *32nd ASME wind energy symposium*: p. 0363. 2014.

[3] Bachynski, Erin E, Kvittem, Marit I, Luan, Chenyu and Moan, Torgeir. "Wind-wave misalignment effects on floating wind turbines: motions and tower load effects." *Journal of Offshore Mechanics and Arctic Engineering* Vol. 136 No. 4 (2014): p. 041902.

[4] Li, Xiuhe, Zhu, Caichao, Fan, Zhixin, Chen, Xu and Tan, Jianjun. "Effects of the yaw error and the wind-wave misalignment on the dynamic characteristics of the floating offshore wind turbine." *Ocean Engineering* Vol. 199 (2020): p. 106960.

[5] Vugts, JH. "Fatigue damage assessments and the influence of wave directionality." *Applied Ocean Research* Vol. 27 No. 3 (2005): pp. 173–185.

[6] Duarte, Tiago, Gueydon, Sébastien, Jonkman, Jason and Sarmento, António. "Computation of wave loads under multidirectional sea states for floating offshore wind turbines." *International conference on offshore mechanics and arctic engineering*, Vol. 45547: p. V09BT09A023. 2014. American Society of Mechanical Engineers.

[7] Allen, Christopher, Viscelli, Anthony, Dagher, Habib, Goupee, Andrew, Gaertner, Evan, Abbas, Nikhar, Hall, Matthew and Barter, Garrett. "Definition of the UMaine VolturnUS-S reference platform developed for the IEA wind 15-megawatt offshore reference wind turbine." Technical report no. National Renewable Energy Lab.(NREL), Golden, CO (United States); Univ. of . . . . 2020.

[8] NREL. "OpenFAST documentation." https://openfast.readthedocs.io/en/dev/index.html (2025). Accessed: November 13, 2025.

[9] Babarit, Aurélien and Delhommeau, Gérard. "Theoretical and numerical aspects of the open source BEM solver NEMOH." *11th European wave and tidal energy conference (EWTEC2015)*. 2015.

[10] Jonkman, Bonnie J. "TurbSim user's guide." Technical report no. National Renewable Energy Lab.(NREL), Golden, CO (United States). 2006.

[11] Lotsberg, Inge. "Background for new revision of DNV-RP-C203 fatigue design of offshore steel structures." *International Conference on Offshore Mechanics and Arctic Engineering*, Vol. 49149: pp. 125–134. 2010.

[12] Palmgren, Arvid. "Die Lev/bensdauer von kugellagern." *VDI. Z.* Vol. 68 (1924): pp. 339–341.

[13] Miner, Milton A. "Cumulative damage in fatigue." (1945).

[14] (IEC), International Electrotechnical Commission. "Wind energy generation systems — Part 1: Design requirements." https://webstore.iec.ch/en/publication/26423 (2019).

[15] Haid, Lorenz, Stewart, Gordon, Jonkman, Jason, Robertson, Amy, Lackner, Matthew and Matha, Denis. "Simulation-length requirements in the loads analysis of offshore floating wind turbines." *International Conference on Offshore Mechanics and Arctic Engineering*, Vol. 55423: p. V008T09A091. 2013. American Society of Mechanical Engineers.

Copyright ©2026 by ASME